CHAPTER IV

RESULTS AND DISCUSSION

PART 1: Effect of boron modification on MCM-41-supported dMMAO/zirconocene catalyst during ethylene/1-octene copolymerization with varied boron loading

In this part, the catalytic activity during ethylene/1-octene copolymerization of B-modified MCM-41-supported dMMAO with a zirconocene catalyst was investigated. In fact, the MCM-41 support was prepared, then sequentially modified with B having approximately 1 and 5 wt% of B in the support, named as 1B-MCM-41 and 5B-MCM41, respectively. The B-modified MCM-41 supports were then characterized using XRD, Raman spectroscopy and SEM/EDX.

MCM-41 was prepared in the same manner as that of Panpranot *et. al.* [59]. It showed the BET surface area, pore volume and pore diameter were 863.51 m^2/g, 0.89 cm^3/g and 3 nm respectively.

4.1 Characterization of supports and catalyst precursors

4.1.1 Characterization of supports and catalyst precursors with X-ray diffraction (XRD)

Typical X-Ray diffraction patterns of MCM-41 usually show four Bragg peaks indicating the long-range order present in this material. The XRD pattern of the MCM-41 prepared with cetyltrimethyl ammonium bromide as template is shown in Figure 4.1. The Bragg peaks can be indexed assuming a hexagonal symmetry.

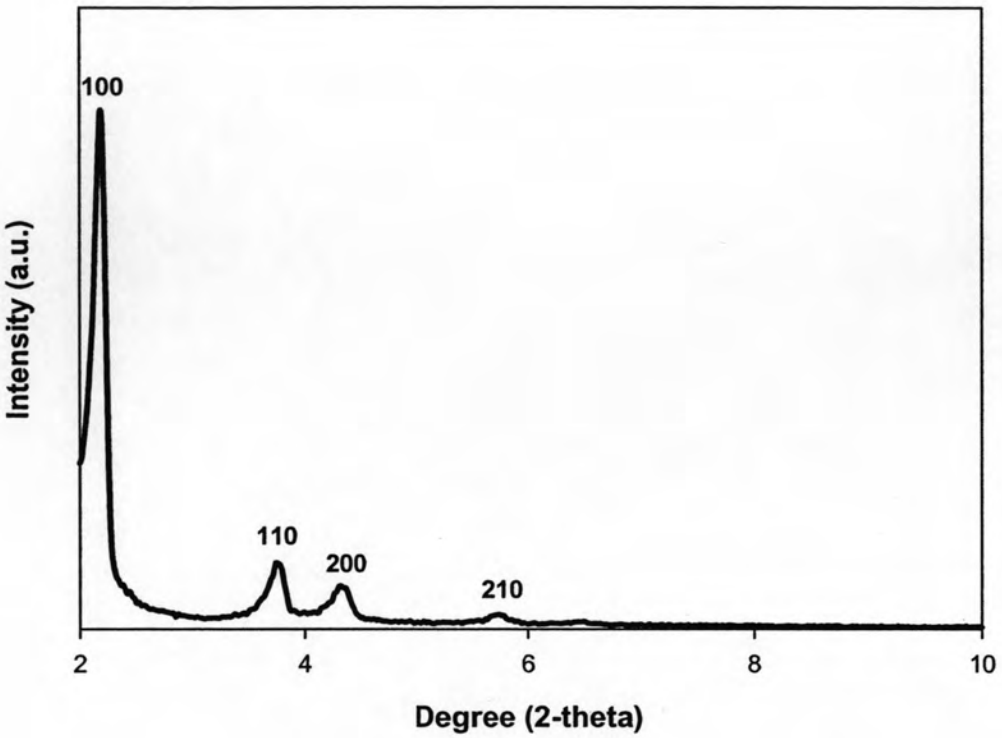

Figure 4.1 XRD pattern of MCM-41 as synthesized.

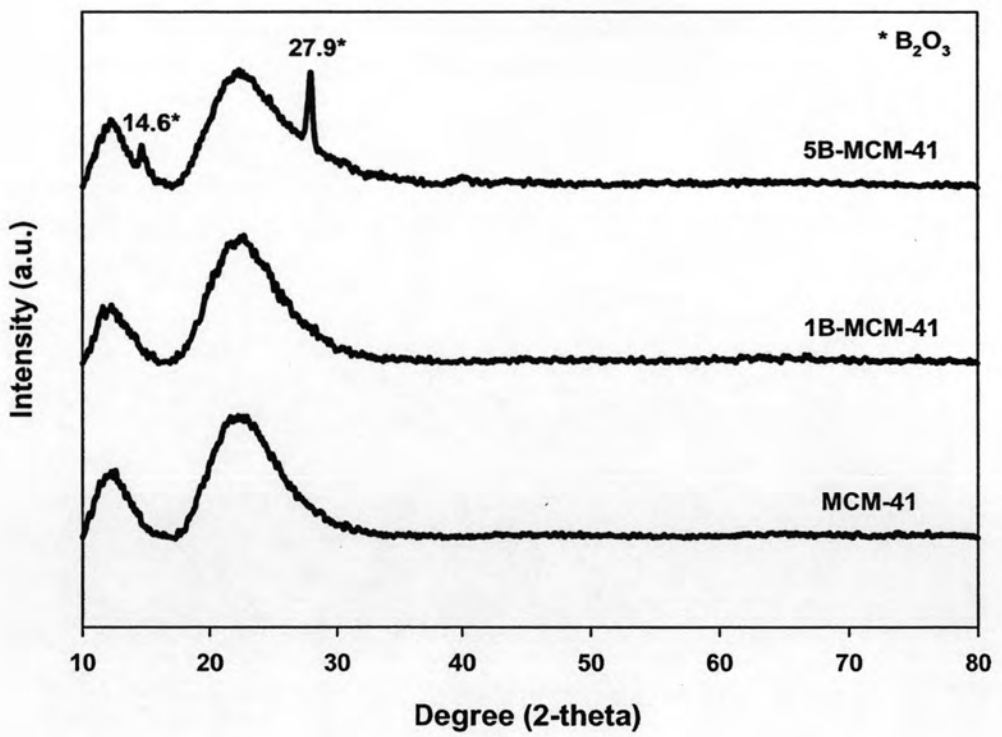

Figure 4.2 XRD pattern of MCM-41 support

The XRD patterns of the unmodified MCM-41 and B-modified MCM-41 supports are shown in Figure 4.2. It can be seen that the unmodified MCM-41 support exhibited the characteristic board peaks of the amorphous silica at ca. 10° to 30°. After modification with 1 wt% of B, the support still exhibited the similar XRD patterns as seen for the unmodified one. It indicated that B_2O_3 was in the highly dispersed form, which was invisible by XRD. However, when increased the B loading to 5 wt%, the XRD peaks of B_2O_3 can be detected at ca. 14.6° (weak) and 27.9° (strong).

4.1.2 Characterization of supports and catalyst precursors with Raman spectroscopy

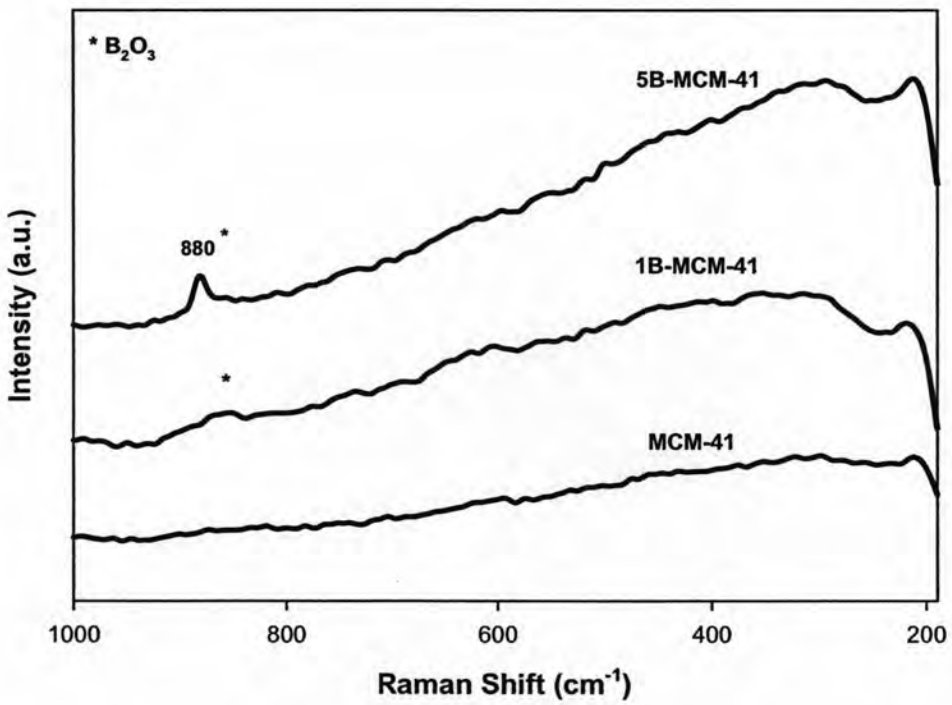

Figure 4.3 Raman spectra of MCM-41 supports

Raman spectra of supports with and without B modification are shown in Figure 4.3. No significant Raman bands were observed for the unmodified MCM-41 support between 200 to 1000 cm^{-1}. However, the strong Raman band for B_2O_3 was observed at ca. 880 cm^{-1} for 5B-MCM-41. For the low (1 wt%) B loading sample, the characteristic Raman band at 880 cm^{-1} was only slightly observed. It should be noted that Raman spectroscopy is more of surface technique. Therefore, the observation of B with

low loading at surface could be possible which was not the case for the bulk as seen by XRD.

4.1.3 Characterization of supports and catalyst precursors with Scanning electron microscope(SEM) and energy dispersive X-ray spectroscopy (EDX)

Scanning electron microscopy was also used to determine the morphology of MCM-41. Figure 4.4 is the SEM micrograph of MCM-41. The image reveals that the MCM-41 particles have the tubular structure.

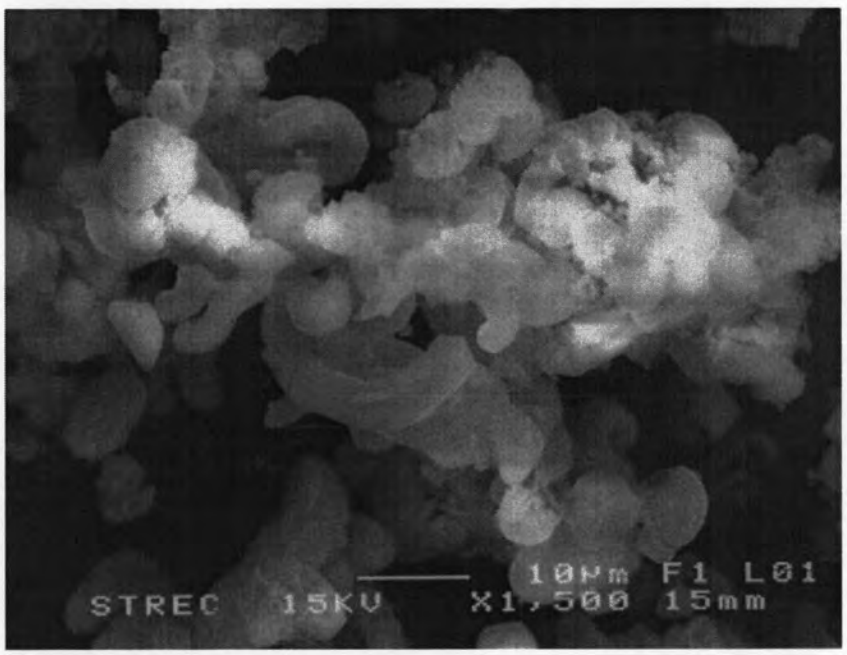

Figure 4.4 SEM micrograph of MCM-41 sample.

The distribution of all elements (Si and Al) obtained from EDX was similar in all samples. The EDX mapping images of the supports can provide more information about the distribution of MMAO as seen for Al distribution mapping on each support. It was found that MMAO was well distributed all over the support granules. The typical EDX mapping images for the MCM-41 supports after impregnation with MMAO are shown in Figure 4.5.

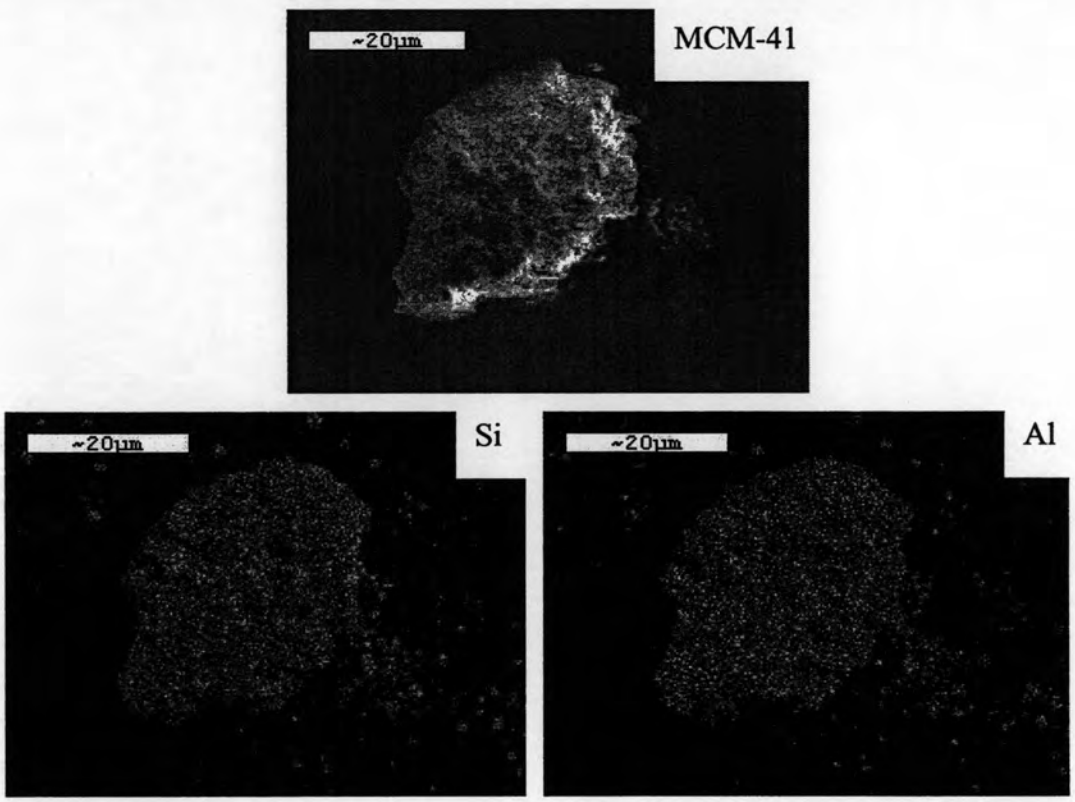

Figure 4.5 EDX mapping of various MCM-41 supports after MMAO impregnation

4.2 Effect of boron-modified MCM-41 supports in ethylene/1-octene copolymerization system

4.2.1 The Effect of boron-modified MCM-41supports on the Catalytic Activity

Table 4.1

Catalytic activities during ethylene/1-octene copolymerization via boron-modified MCM-41-supported-MMAO with zirconocene catalyst

System	Wt% of boron in support	Polymerization time (s)	Polymer yield [a] (g)	Catalytic activity [b] (kg polymer mol^{-1}Zr.h)
Homogeneous	0	82.2	1.6760	48934
MCM-41	0	154.2	1.4314	22279
1B-MCM-41	1	93.0	1.4717	37979
5B-MCM-41	5	91.2	1.3513	35561

[a] The polymer yield was fixed [limited by ethylene fed and 1-octene used (0.018 mole equally)].
[b] Activities were measured at polymerization temperature of 70^0 C, [Ethylene]=0.018 mole, $[Al]_{MMAO}/[Zr]$ = 1135, $[Al]_{TMA}/[Zr]$ = 2500, in toluene with total volume = 30 ml, and [Zr]= $5x10^{-5}$ M

After the impregnation of dMMAO onto the unmodified and B-modified MCM-41 supports, the ethylene/1-octene copolymerization with *rac*-Et$[Ind]_2ZrCl_2$ catalyst was performed in the presence of supports at the same condition for a comparative study regards to the catalytic activities derived from different supports. In fact, the activation of a zirconocene catalyst with methylaluminoxane compound has been reported elsewhere [62]. The activities of catalyst via various supports are listed in Table 4.1. It was obvious that the homogeneous catalytic system provided the highest activity among the supported catalytic system due to the absence of support interaction. Considering the supported system, it can be observed that the B-modified MCM-41 exhibited higher activity than the unmodified MCM-41 almost 2 times for both the 1B-MCM-41 and 5B-MCM41 supports. It should be noted that an increase in the amount of B loading apparently resulted in a slight decrease in the catalytic activity.

In order to determine the effect of B modification, XPS measurement on the various supports was conducted. The binding energy (BE) for B 1s and Al 2p along with the surface concentrations of $[B]_{Support}$ and $[Al]_{dMMAO}$ were measured. The XPS profiles (not shown) for the typical B 1s (BE ~ 192.5-192.8 eV) and Al 2p (BE ~ 74.6-74.8 eV) on various supports in this study were similar. It should be mentioned that the BE of Al 2p was also in accordance with those on silica reported by Shiono group [63]. This was suggested that no significant change in the oxidation state of B (support) and Al (dMMAO) upon the various supports employed. The surface concentrations of $[B]_{Support}$ and $[Al]_{dMMAO}$ measured by XPS are shown in Table 4.2. Considering the surface concentrations of B in different modified supports, it was found that for 1B-MCM-41, boron (~ 1.2 wt% at surface) was mostly located on the surface of MCM-41 whereas most of B was in the bulk for the 5B-MCM-41 indicating that only one forth of B (only 1.3 wt% at surface) was located at surface. The surface concentrations of Al as shown in Table 4.2 were also varied upon the different supports employed. It can be observed that the surface concentrations for the unmodified and 1B-MCM-41 supports were similar (~26.5-26.8 wt%). Although they had the equal amount of Al concentration at surface, the 1B-MCM-41 exhibited dramatically higher activity than the unmodified MCM-41 support almost 2 times. This indicated that B modification would result in a decreased interaction between the support and dMMAO. As a result, activity pronouncedly increased with B modification. However, with increased B loading in the support (5B-MCM-41), the surface concentration of Al apparently decreased significantly. This was presumably due to the migration of Al into the B layer. The lesser amount of surface concentrations of Al would be the main reason for the decreased activity observed in the 5B-MCM-41 support compared to the 1B-MCM-41 support. It was worth noting that even though the surface concentration of $[Al]_{dMMAO}$ for the unmodified MCM-41 support was essentially higher than that of the 5B-MCM-41, the unmodified MCM-41 support exhibited such a lower activity. This was suggested that the stronger support interaction in the unmodified MCM-41 support played more important role on the decreased activity than the amount of dMMAO at surface did. Hence, the unmodified MCM-41 gave lower activity than the 5B-MCM-41 (lesser amount of $[Al]_{dMMAO}$ at surface) did. On the other hand, strong support interaction was the key factor (not the surface concentrations of $[Al]_{dMMAO}$) to determine the catalytic activity for this catalytic system. It can be proposed that B can act as a spacer to anchor the support and dMMAO leading to fewer interactions. In order to give a better understanding for the effect of B modification on

surface concentrations and strong support interaction as mentioned earlier, the suggested model is also illustrated as shown in Figure 4.6.

Table 4.2

XPS results for MCM-41supports

Support	BE for B^{3+} (eV)	BE for Al^{3+} (eV)	Atomic Conc. %		Mass Conc. %	
			B	Al	B	Al
1B-MCM-41	193.973	-	1.48	-	0.87	-
5B-MCM-41	194.447	-	9.28	-	5.75	-
dMMAO	-	74.615	-	23.41	-	30.11
MCM-41/dMMAO	-	74.734	-	20.44	-	26.49
1B-MCM-41/dMMAO	192.517	74.842	2.20	20.20	1.17	26.81
5B-MCM-41/dMMAO	192.812	74.832	2.26	13.99	1.26	19.41

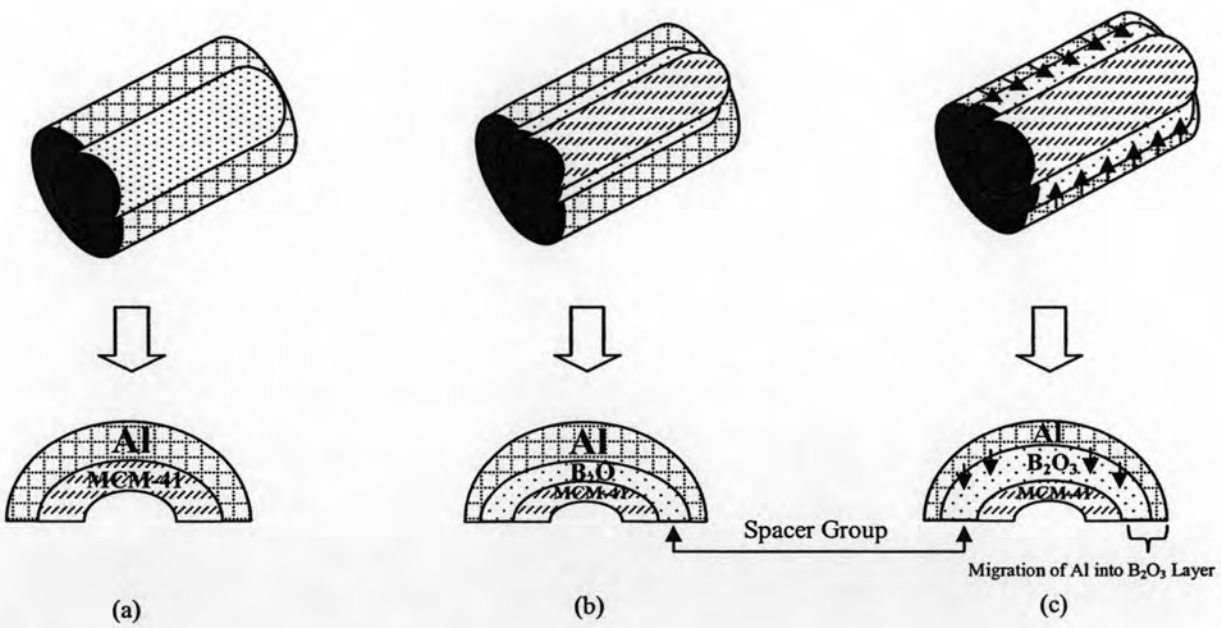

Figure 4.6 Suggested model in role of boron on MCM-41-supported

The TGA measurement was performed to proof the interaction between the $[Al]_{dMMAO}$ and various supports. The TGA profiles of $[Al]_{dMMAO}$ on various supports are shown in Figure 4.7 indicating the similar profiles for various supports. It was observed that the weight loss of $[Al]_{dMMAO}$ present on various supports were in the order of 5B-MCM-41 (20%) > 1B-MCM-41 (17%) > MCM-41 (13%). The species having strong interaction with the support was removed at ca. 280, 290 and 333 ^{0}C for 5B-MCM-41, 1B-MCM-41 and MCM-41, respectively. This indicated that $[Al]_{dMMAO}$ present on MCM-41 without B modification had the strongest interaction, thus, lowest polymerization activity was observed.

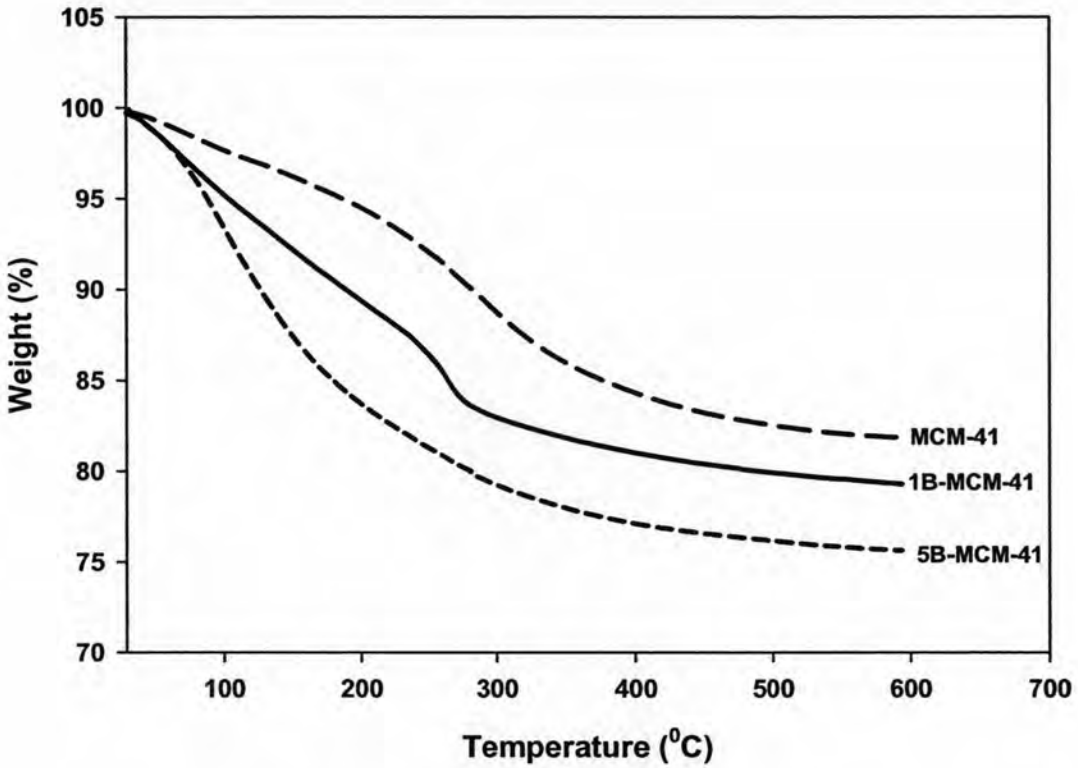

Figure 4.7 TGA result of MCM-41 supports

4.2.2 The Effect of boron-modified MCM-41 supports on the molecular weight of copolymers

The molecular weight based on weight average (M_w) and based on number average (M_n), and molecular weight distribution (MWD) of polymers obtained by a gel permeation chromatography are shown in Table 4.3. and GPC curves of the copolymer are also shown in Appendix C.

Table 4.3

Molar weight and molecular weight distribution of polymers obtained via boron-modified MCM-41-supported-MMAO with zirconocene catalyst

System	M^a_w ($x10^{-4}$ g mol^{-1})	M^a_n ($x10^{-4}$ g mol^{-1})	MWD^a
Homogeneous	2.13	0.63	3.4
MCM-41	2.15	0.63	3.4
1%B-MCM-41	2.61	1.02	2.6
5%B-MCM-41	2.42	1.45	1.7

[a] Obtained from GPC and MWD was calculated from M_w/M_n.

The MW and MWD of polymer obtained from different supports are shown in Table 4.3. Based on the GPC curve (see Appendix C), only the unimodal molecular weight distribution of polymer was obtained. It can be observed that B modification apparently resulted in a slight increase in MW of polymer produced. This was suggested that inhibition of chain transfer reaction during polymerization could be achieved with the B modification on MCM-41 support. Furthermore, it was worth noting that the narrower MWD was also evident for B modification indicating more uniform catalytic sites occurred.

4.2.3 The Effect of B-modified MCM-41 supports on the incorporation of polymers

Table 4.4

Triad distribution obtained by ^{13}C NMR measurement of ethylene (E) and 1-octene (O) in polymers produced

System	Wt % of boron in support	OOO	EOO	EOE	EEE	OEE	OEO
Homogeneous	0	0	0.100	0.154	0.481	0.228	0.045
MCM-41	0	0	0.024	0.127	0.583	0.245	0.032
1B-MCM-41	1	0	0.077	0.130	0.614	0.177	0.041
5B-MCM-41	5	0	0.075	0.136	0.597	0.174	0.034

It has been known that ^{13}C NMR is one of the most powerful techniques to identify the polymer microstructure, especially polyolefins [65]. The resulted ^{13}C NMR spectra (see Appendix A) for all samples were assigned typically to the copolymers obtained from copolymerization of ethylene/1-octene. The triad distribution was identified based on the method described by Randall [61]. It can be observed that the produced copolymers exhibited similar ^{13}C NMR patterns indicating similar molecular structure of polymer. Based on calculations described by Galland et. al. [64], the triad distribution of monomer is listed in Table 4.4. It showed that B modification resulted in slightly increased % octene incorporation. No block OOO was observed.

Table 4.5

Reactivity ratios of ethylene (r_E) and 1-octene (r_O) calculated from ^{13}C NMR measurement

System	Wt % of boron in support	Incorporation (%)		Reactivity ratios ($r_E r_O$)
		E	O	
Homogeneous	0	75	25	0.90
MCM-41	0	85	15	0.39
1B-MCM-41	1	80	20	1.21
5B-MCM-41	5	79	21	1.18

When considered the results in Table 4.5, the MCM-41 supports modified with B gave an increase in the % incorporation of 1-octene in the produced polymer containing block copolymer ($r_E r_O > 1$).

4.2.4 The Effect of boron modified MCM-41 supports on the melting temperatures of copolymers

Table 4.6

Thermal properties of polymers obtained from DSC measurement

System	Wt % of boron in support	1-octene insertion [a] (%)	T_m (^{0}C)	ΔH_m (J/g)	%Crystallinity (%χ)
Homogeneous	0	25	85.68	1.9261	0.67
MCM-41	0	15	70.91	3.5820	1.25
1B-MCM-41	1	20	80.22	6.6884	2.34
5B-MCM-41	5	21	82.50	3.6141	1.26

[a] 1-octene insertion or incorporation was calculated based on ^{13}C NMR.

It has been known that the melting temperature (T_m) trended to decrease with more insertion of comonomer due to decreased crystallinity [65]. On the contrary, the melting temperature (T_m) trended to increase with less insertion of comonomer due to increased crystallinity. However, the melting temperature (T_m) as shown in Table 4.6 trended to decrease with the decreased insertion of 1-octene due to increased crystallinity. This should be addressed that besides the effect of 1-octene insertion on the T_m, the MCM-41 added also affected the T_m of polymer as well. Moreover, it was found that B added also affected the T_m of polymer, the insertion of 1-octene and crystallinity. It was reported that the particles in polymer matrix can act as nucleating agents [65]. Consequently, they increase the crystallinity of polymer. Apparently, whereas higher 1-octene insertion resulted in higher T_m and crystallinity. However, it was found that at higher content of B in polymer rendered lower crystallinity.

PART 2: Effect of boron modification on MCM-41-supported dMMAO/zirconocene catalyst during ethylene/1-octene copolymerization on the different pore size of MCM-41 supports with varied boron loading

In this part, the catalytic activity during ethylene/1-octene copolymerization of B-modified MCM-41-supported dMMAO with a zirconocene catalyst on the different pore sizes of MCM-41 supports with various boron loading were investigated. In fact, the MCM-41 support was prepared in both small pore and large pore, then sequentially modified with B having approximately 1 and 5 wt% of B in the support, named as 1BS-MCM-41 and 5BS-MCM-41 for MCM-41 small pore and 1BL-MCM-41 and 5BL-MCM-41 for MCM-41 large pore, respectively. The B-modified MCM-41 supports were then characterized using XRD, Raman spectroscopy and SEM/EDX.

MCM-41 was prepared in the same manner as that of Panpranot *et. al.* [59]. It showed the BET surface area, pore volume and pore diameter were 863.51 m^2/g, 0.89 cm^3/g and 3 nm, respectively for MCM-41 small pore (from part 1) and BET surface area, pore volume and pore diameter were 290.38 m^2/g, 0.87 cm^3/g and 9 nm, respectively for MCM-41 large pore.

4.3 Characterization of supports and catalyst precursors

4.3.1 Characterization of supports and catalyst precursors with X-ray diffraction (XRD)

It can be observed that XRD patterns of MCM-41 for both small pore and large pore were similar as shown in Figure 4.8. The XRD results were also mentioned in 4.1.1.

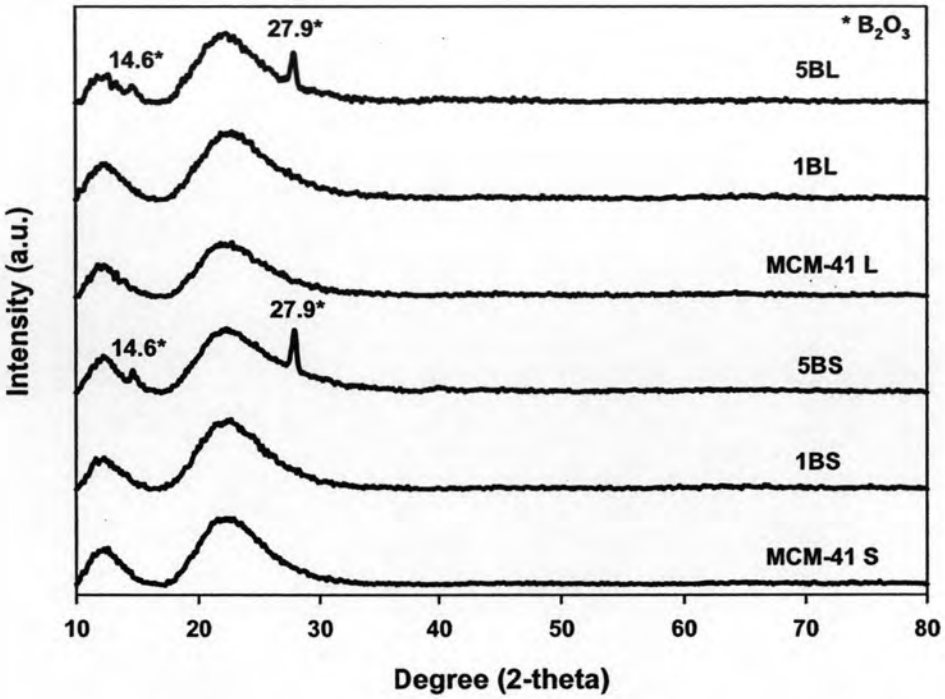

Figure 4.8 XRD pattern of various MCM-41 supports

4.3.2 Characterization of supports and catalyst precursors with Raman spectroscopy

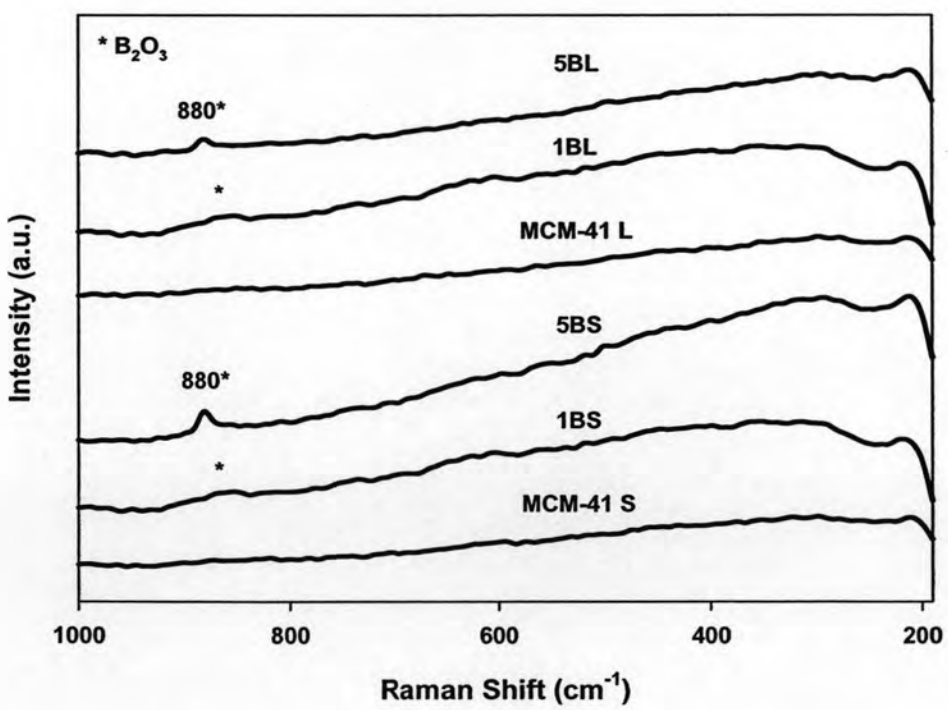

Figure 4.9 Raman spectra of various MCM-41 supports

It can be observed that Raman spectra of MCM-41 for both small pore and large pore were similar as shown in Figure 4.9. The Raman spectroscopy results were also mentioned in 4.1.2.

4.3.3 Characterization of supports and catalyst precursors with Scanning electron microscope (SEM) and energy dispersive X-ray spectroscopy (EDX)

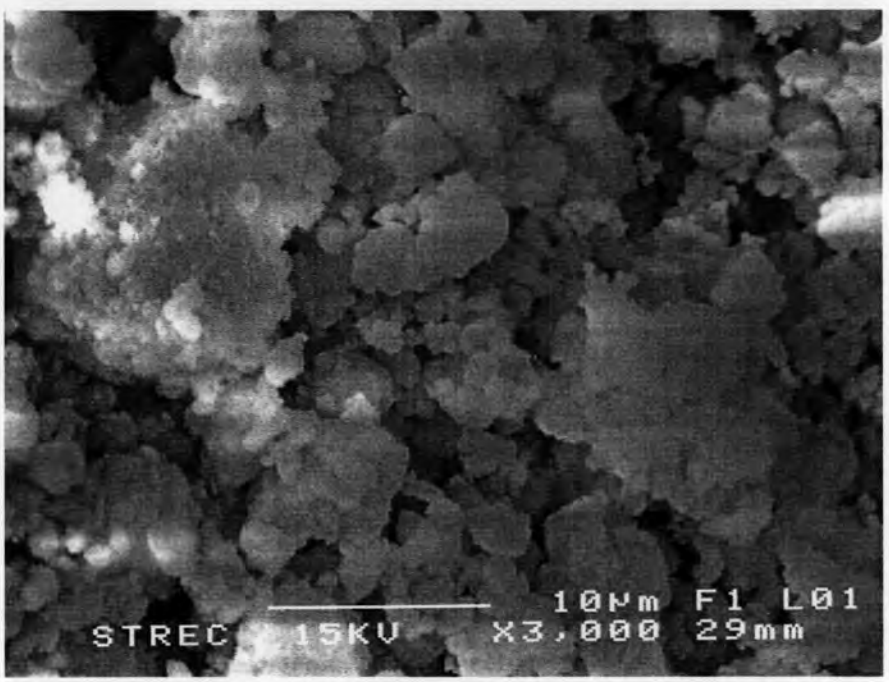

Figure 4.10 SEM micrograph of MCM-41 large pore support

The MCM-41 having large pore was originally prepared from the MCM-41 having small pore by treating it with *N, N*-dimethyldecylamine caused MCM-41 changed the morphology. Therefore, the SEM micrograph of MCM-41 large pore was apparently different from those of MCM-41 small pore (Figure 4.4).

The distribution of all elements (Si and Al) obtained from EDX was similar in all samples. The EDX mapping images of the supports can provide more information about the distribution of MMAO as seen for Al distribution mapping on each support. It was found that MMAO was well distributed all over the support granules. The typical EDX mapping images for the MCM-41 supports after impregnation with MMAO are shown in Figure 4.11.

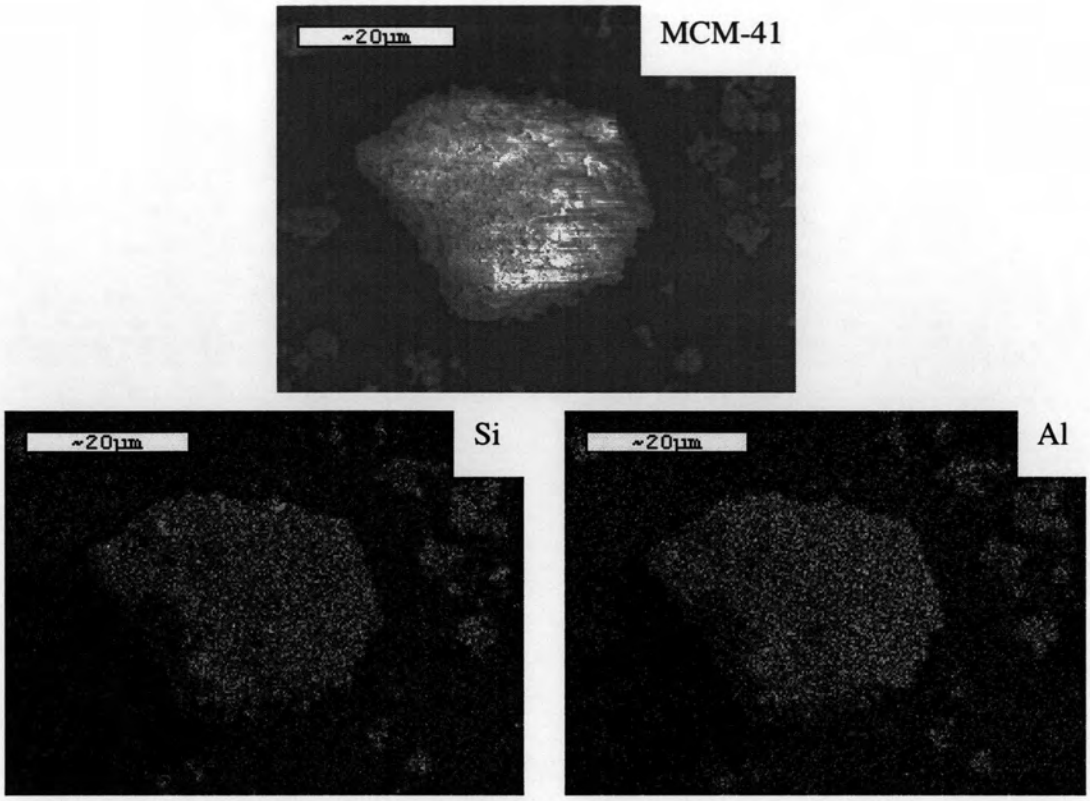

Figure 4.11 EDX mapping of various MCM-41 large pore supports after MMAO impregnation

4.4 Effect of boron-modified MCM-41 supports with different pore size in ethylene/1-octene copolymerization system

4.4.1 The Effect of boron-modified MCM-41supports on the catalytic activity

Table 4.7

Catalytic activities during ethylene/1-octene copolymerization via boron-modified MCM-41-supported-MMAO with zirconocene catalyst with different pore size

System	Wt % of boron in support	Polymerization time (s)	Polymer yield [a] (g)	Catalytic activity [b] (kg polymer mol^{-1}Zr.h)
Homogeneous	0	82.2	1.6760	48934
MCM-41 S[c]	0	154.2	1.4314	22279
1B[d]-MCM-41 S	1	93.0	1.4717	37979
5B[e]-MCM-41 S	5	91.2	1.3513	35561
MCM-41 L[f]	0	94.2	1.0234	26073
1B-MCM-41 L	1	121.2	1.3216	26170
5B-MCM-41 L	5	126.6	1.5417	29227

[a] The polymer yield was fixed [limited by ethylene fed and 1-octene used (0.018 mole equally)].
[b] Activities were measured at polymerization temperature of 70 ^{0}C, [Ethylene]=0.018 mole, $[Al]_{dMMAO}/[Zr]_{cat}$ = 1135, $[Al]_{TMA}/[Zr]_{cat}$ = 2500, in toluene with total volume = 30 ml, and $[Zr]_{cat} = 5x10^{-5}$ M.
[c] Refers to MCM-41 small pore.
[d] Refers to loading of 1 wt% boron on the MCM-41-support.
[e] Refers to loading of 5 wt% boron on the MCM-41-support.
[f] Refers to MCM-41 large pore.

Considering the results in Table 4.7, after the impregnation of dMMAO onto the unmodified and B-modified MCM-41 supports, the ethylene/1-octene copolymerization with *rac*-Et[Ind]$_2$ZrCl_2 catalyst was performed in the presence of supports at the same condition for a comparative study regards to the catalytic activities derived from different supports. It was obvious that the homogeneous catalytic system provided the highest activity among the supported catalytic system due to the absence of support interaction. The activity results of ethylene/1-octene copolymerization for the MCM-41 small pore supports were already mentioned as in 4.2.1.

Considering, activities of ethylene/1-octene copolymerization as listed in Table 4.7, for the MCM-41 large pore system, it was found that the 5B-MCM-41 having large pore exhibited higher activity than the 1B-MCM-41 and MCM-41 large pore, respectively, but it was slightly different between unmodified and B-modified MCM-41 supports. From such a point of view, it can be seen that the MCM-41 small pore system gave higher activities than that of the MCM-41 large pore system. This can be attributed to the dispersion and interaction between $[Al]_{MMAO}$ and supports.

The TGA measurement was performed to proof the interaction between the $[Al]_{dMMAO}$ and various supports. The TGA profiles of $[Al]_{dMMAO}$ on various supports are shown in Figure 4.12 indicating the similar profiles for various supports. It was observed that the weight loss of $[Al]_{dMMAO}$ present on various supports were in the order of 1B-MCM-41L (22%) > 5B-MCM-41L (19%) > MCM-41L (18%). The species having strong interaction with the support was removed at ca. 406, 418 and 432 ^{0}C for 1B-MCM-41, 5B-MCM-41 and MCM-41, respectively. This indicated that $[Al]_{dMMAO}$ present on MCM-41 without B modification had the strongest interaction, thus, lowest polymerization activity was observed.

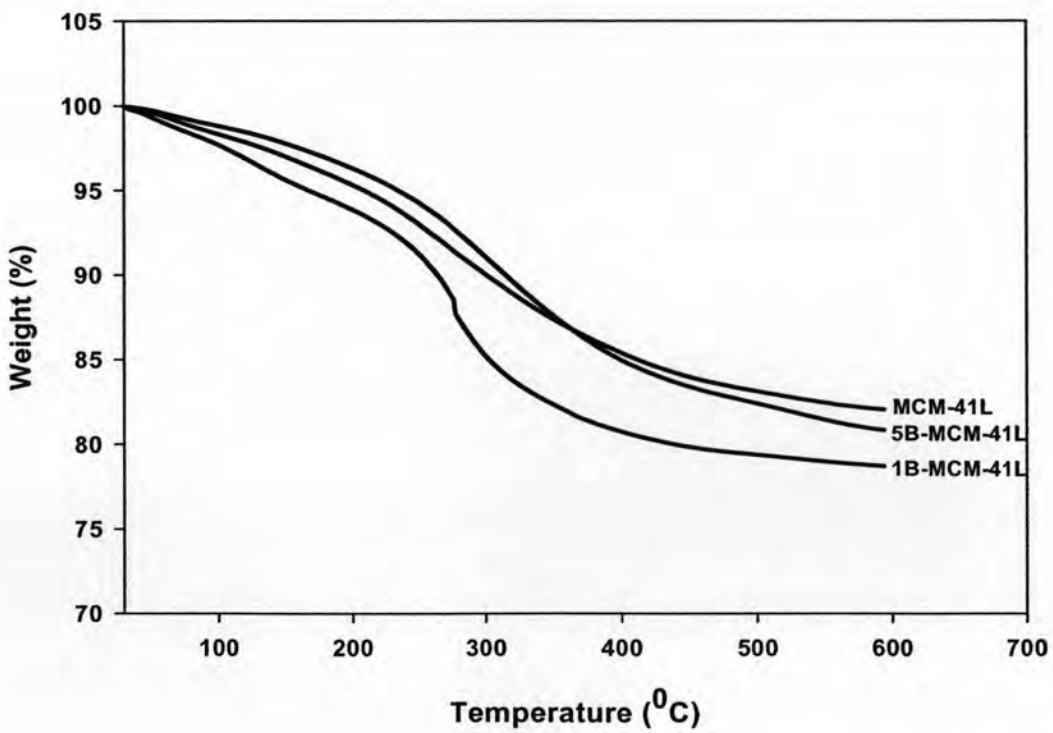

Figure 4.12 TGA result of various MCM-41 large pore supports

Table 4.8

Weight loss of $[Al]_{dMMAO}$ in MCM-41 and average amount of $[Al]_{dMMAO}$ in MCM-41

Sample	Temperature [a] (^{0}C)	Weight loss [a] (%)	% Al from EDX
MCM-41 Small Pore/dMMAO	333	13	10.79
1B-MCM-41 Small Pore/dMMAO	290	17	11.94
5B-MCM-41 Small Pore/dMMAO	280	20	13.34
MCM-41 Large Pore/dMMAO	432	18	9.46
1B-MCM-41 Large Pore/dMMAO	406	22	11.72
5B-MCM-41 Large Pore/dMMAO	418	19	12.11

[a] Obtained from TGA measurement

Considering the weight loss of $[Al]_{dMMAO}$ in MCM-41 between MCM-41 having small pore and large pore system as shown in Table 4.8, it showed that the weight loss of $[Al]_{dMMAO}$ in MCM-41 having large pore system was higher than that of small pore system indicating weaker interaction of the support and $[Al]_{dMMAO}$. However, when considered the activity achieved in Table 4.7, it can be expressed that the MCM-41 having large pore system gave lower activity than the small pore system one. From this result, EDX measurement was used to describe this phenomenon. From Table 4.8, it can be observed that the amount of $[Al]_{dMMAO}$ in MCM-41 having small pore system was higher than that of MCM-41 large pore system resulting in higher activities. It seems reasonable to suppose that the higher amounts of $[Al]_{dMMAO}$ in MCM-41 small pore system remarkably affected on the higher activity than the interaction between the support and cocatalyst.

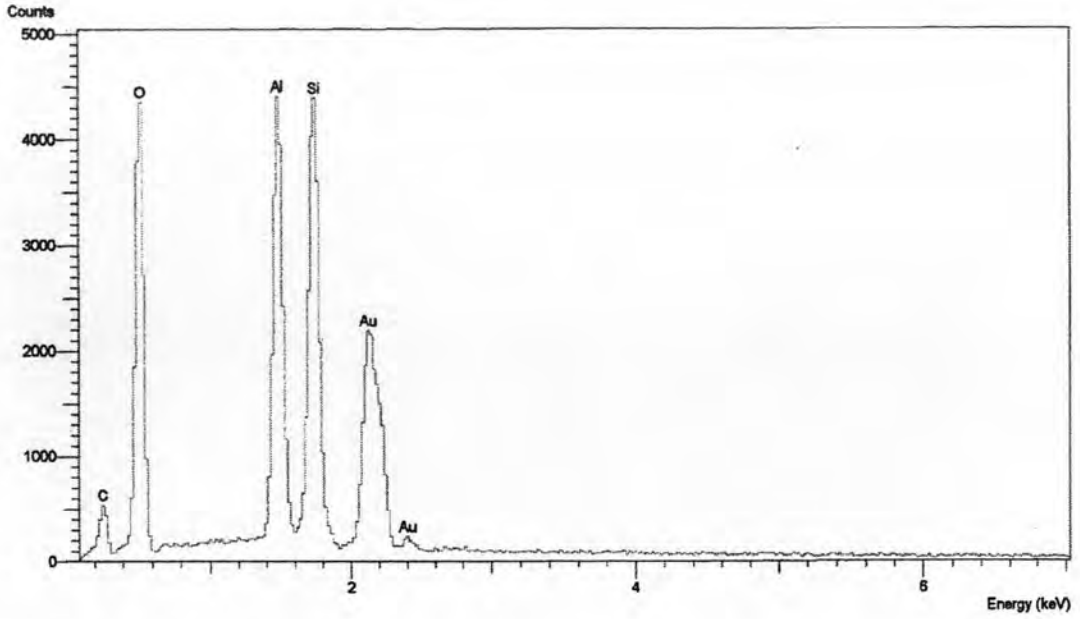

Figure 4.13 A typical spectrum of the supported dMMAO from EDX analysis used to measure the average [Al]dMMAO concentration on various supports

The typical measurement curve for the quantitative analysis using EDX is shown in Figure 4.13. It can be seen that the amounts of $[Al]_{dMMAO}$ in various supports were varied due to the adsorption ability of each support. Besides the content of $[Al]_{dMMAO}$ in supports, one should consider the distribution of $[Al]_{dMMAO}$ in the supports. The elemental distribution was also performed using EDX mapping on the external surface and were also mentioned in 4.1.3 and 4.3.3.

4.4.2 The Effect of boron-modified MCM-41 supports with different pore size on the molecular weight of copolymers

The molecular weight based on weight average (M_w) and based on number average (M_n), and molecular weight distribution (MWD) of polymers obtained by a gel permeation chromatography are shown in Table 4.9 and GPC curves of the copolymer are also shown in Appendix C.

Table 4.9

Molar weight and molecular weight distribution of polymers obtained via boron-modified MCM-41-supported-MMAO with zirconocene catalyst

System	M^a_w ($x10^{-4}$ g mol^{-1})	M^a_n ($x10^{-4}$ g mol^{-1})	MWD[a]
Homogeneous	2.13	0.63	3.4
MCM-41 Small Pore	2.15	0.63	3.4
1%B-MCM-41 Small Pore	2.61	1.02	2.6
5%B-MCM-41 Small Pore	2.42	1.45	1.7
MCM-41 Large Pore	4.10	1.80	2.3
1%B-MCM-41 Large Pore	2.54	1.95	1.3
5%B-MCM-41 Large Pore	2.79	0.53	5.3

[a] Obtained from GPC and MWD was calculated from M_w/M_n.

The MW and MWD of polymer obtained from different supports are shown in Table 4.9. Based on the GPC curve (see Appendix C), only the unimodal molecular weight distribution of polymer was obtained. For the MCM-41 having small pore system, it can be observed that the B modification apparently resulted in a slight increase in MW of polymer produced. This was suggested that inhibition of chain transfer reaction during polymerization could be achieved with the B modification on MCM-41 support. Furthermore, it was worth noting that the narrower MWD was also evident for B modification indicating more uniform catalytic sites occurred. For the MCM-41 having large pore system, the results of MW and MWD were opposite to the MCM-41 small pore system. It was obvious that B modification apparently resulted in a decrease in MW of polymer produced. Considering MWD, it showed that the narrower MWD was evident for B modification at low content of B indicating more uniform catalytic sites occurred. But at higher content of B, it showed the broad MWD indicating less single site occurred.

4.4.3 The Effect of boron-modified MCM-41 supports on the incorporation of polymers

Table 4.10

Triad distribution obtained by ^{13}C NMR measurement of ethylene (E) and 1-octene (O) in polymers produced

Systems	Wt % of boron in support	OOO	EOO	EOE	EEE	OEE	OEO
Homogeneous	0	0	0.100	0.154	0.481	0.228	0.045
MCM-41 S	0	0	0.024	0.127	0.583	0.245	0.032
1B-MCM-41 S	1	0	0.077	0.130	0.614	0.177	0.041
5B-MCM-41 S	5	0	0.075	0.136	0.597	0.174	0.034
MCM-41 L	0	0	0.025	0.107	0.713	0.156	0.012
1B-MCM-41 L	1	0	0.113	0.139	0.519	0.179	0.053
5B-MCM-41 L	5	0	0.105	0.135	0.488	0.236	0.041

The triad distribution of the MCM-41 having small pore and large pore system is shown in Table 4.10. The description of triad distribution of the MCM-41 having large pore system were similar to the MCM-41 small pore system as mentioned above in 4.2.3.

Table 4.11

Reactivity ratios of ethylene (r_E) and 1-octene (r_O) calculated from ^{13}C NMR measurement

System	Wt % of boron in support	Incorporation (%)		Reactivity ratios ($r_E r_O$)
		E	O	
Homogeneous	0	75	25	0.90
MCM-41 S	0	85	15	0.39
1B-MCM-41 S	1	80	20	1.21
5B-MCM-41 S	5	79	21	1.18
MCM-41 L	0	87	13	0.92
1B-MCM-41 L	1	75	25	1.20
5B-MCM-41 L	5	76	24	1.06

When considered % incorporation of 1-octene and reactivity ratios as listed in Table 4.11, for both MCM-41 having small pore and large pore modified with boron gave an increase in the %incorporation when compared to the unmodified MCM-41. It was obvious that the modified MCM-41 for both small pore and large pore with B gave block copolymer ($r_E r_O > 1$)

Table 4.12

Thermal properties of polymers obtained from DSC measurement

System	Wt % of boron in support	1-octene insertion [a] (%)	T_m (^{0}C)	ΔH_m (J/g)	%Crystallinity (%χ)
Homogeneous	0	25	85.68	1.9261	0.67
MCM-41 S	0	15	70.91	3.5820	1.25
1B-MCM-41 S	1	20	80.22	6.6884	2.34
5B-MCM-41 S	5	21	82.50	3.6141	1.26
MCM-41 L	0	13	75.73	6.1381	2.15
1B-MCM-41 L	1	25	-[b]	4.1943	1.47
5B-MCM-41 L	5	24	-[b]	1.9856	0.69

[a] 1-octene insertion or incorporation was calculated based on ^{13}C NMR.

[b] Value not be detected from the measurement

The thermal properties such as T_c and T_m obtained from DSC measurement along with % crystallinity are summarized in Table 4.12. It was found that for both MCM-41 having small pore and large pore system gave the melting temperature (T_m) as shown in Table 4.12 trended to decrease with the decreased insertion of 1-octene due to increased crystallinity. This should be addressed that besides the effect of 1-octene insertion on the T_m, the MCM-41 added also affected the T_m of polymer as well. Considering the MCM-41 having small pore system, it was found that B added also affected the T_m of polymer, the insertion of 1-octene and crystallinity. Apparently, while higher 1-octene insertion resulted higher T_m and crystallinity. However, at higher content of B in polymer rendered lower crystallinity. Oppositely, the MCM-41 having large pore system, while higher 1-octene insertion resulted in decreased crystallinity and no T_m was observed.